Experimental and Analytical Investigation on Operating Characteristics for an Ejector Ramjet

Keiichi OKAI, Hideyuki TAGUCHI and Hisao FUTAMURA
Institute of Space Technology and Aeronautics, Japan Aerospace Exploration Agency
7-44-1 Jindaiji-Higashi Chofu Tokyo 182-8522 Japan
Email: okai.keiichi@jaxa.jp

Keywords: Ejector, One-dimensional analysis, Mixing

Abstract

Experiments and numerical calculations were conducted on the flow field of a model ejector ramjet configuration to investigate fundamental fluid dynamic aspects of its pumping and mixing effects. Also a one-dimensional flight performance analysis program was constructed with a simple ejector modeling. After comparing the model with some of the previous experimental and numerical results, a flight performance analysis was conducted with the program. The present states of the program and some features to be improved are presented.

Nomenclature

A: Area
D: Dimension of primary flow exit [mm]
CFD: Computational Fluid Dynamics
DAB: Diffusion and after burn
H: Duct height [mm], Altitude [km]
H_2: Hydrogen
Isp: Specific impulse [s]
L: Mixing duct length [mm]
M: Mach number
OE: Over expansion
P: pressure [MPa]
q: Dynamic pressure [kPa]
RANS: Reynolds-Averaged Navier-Stokes
RBCC: Rocket Based Combined Cycle
SMC: Simultaneous mixing and combustion
UE: Under expansion
x: Stream-wise length along the duct from the primary nozzle exit [mm]
α: Mass flow ratio ($=m_s/m_p$)
ψ: Thrust augmentation ratio (thrust of whole ejector system divided by imaginary rocket alone thrust)

Subscripts
amb: Ambient
e: Exhaust plane
i: Inlet plane
m: (Mixing region) exit plane
p: Primary
s: Secondary
t: Total
w: Wall
0: Ambient, standard
*: Throat

Introduction

After the maturity of the rocketry, some of the more reliable, robust and low cost vehicle configurations for space transportations are wanted. For many years combined cycle engines with airbreathing engine(s) have been studied for the purpose. Recently several integration studies of the combined Cycle Engines are re-focused on by many institutes [1], as the progresses have been made on fundamental key technologies such as supernosinc combustion [2].

Ejector ramjet concept itself is quite simple and classical as is seen in a textbook [3]. However, these previous studies on experiment, CFD and simple flight performance analysis were not well combined and evaluated in a unified fashion. The Ejector Ramjet is a concept for utilization of a relatively low speed-region accelerator as ramjet can not be operated for those speed ranges. For those lower speed conditions, the ejector rocket serves as a pumping device to entrain surrounding air by shear and suction forces. The ejector ramjet is promising as low speed mode of the RBCC engine having simple structure and possibly lighter weitht than introduction of other engine modes, although the ejector-system performance would be lower than other low speed engines such as turbojet engines. The ejector configuration with supersonic pumping jet is widely used such as vacuum pump and chemical lasers [4]. Recent progress in this area is outstanding, including several systematic combustion testings by NASA Glenn [5] and JAXA [6]. In parallel, fundamental studies have been conducted by many researchers but those results are not utilized in a systematic point of view, as explained above.

From the background, the authors have been conducted an experimental and numerical study on a

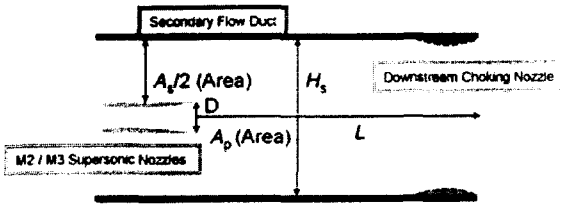

Figure 1. Geometry of the test apparatus.

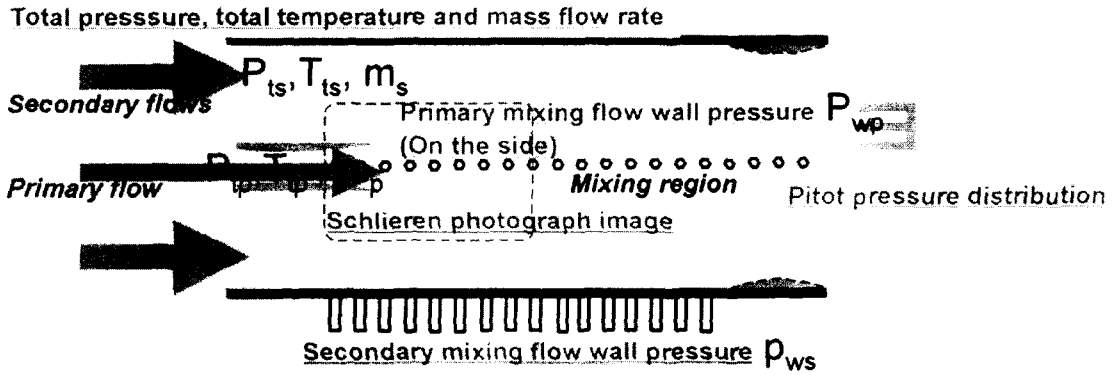

Figure 2. Observation and measurement plan of the flow-field testing of the model ejector ramjet configuration.

model ejector ramjet configuration to investigate the pumping and mixing characteristics of it [7, 8]. Succeedingly the authors have started construction of a simple analytical program for attainment of a flight performance of the ejector ramjet configuration. As the first step, the analytical model was made so that comparison with previous related work and evaluation can be made. The present paper reports the evaluation of the classical analysical modeling by comparing the result with our previous experimental and numerical investigations. Also the program was applied to a sample flight condition to show the validity of the current approach. Finally some features to be overcome for more precise and reliable performance analysis are proposed.

Present Study Procedure and Conditions

Experiment

A series of aerodynamic experiment and a corresponding CFD analysis were conducted. Aiming at related analytical investigation and flow visualization, the geometrical formulation of the test apparatus is a simple quasi-two-dimensional parallel shape one. Figure 1 shows a schematic of the experimental setup. The whole apparatus is installed in a low pressure chamber to controll the ambient pressure and the primary and secondary flows are feeded from the upstream ducts. The primary flow is provided as a pressurized and heated air by a compressor and an electric heater. Basic configuration of the primary flow feeding system and a low pressure chamber is similar to the test configuretion used by Taguchi and co-workers [9]. The primary flow test conditions controlled are total pressure P_{tp} and total temperature T_{tp}, and the mass flow of the primary flow m_p was measured using a V cone flow meter (differrential flow meter). The secondary flow is introduced from surrounding (ambient) air or as a branch flow from the primary pressurized flow duct. The secondary flow total temperature is the atmospheric temperature and mass flow rate (or total pressure) of the secondary flow is controlled by an electromagnetic valve. Measured properties of the secondary flow are total pressure P_{ts}, total temperature T_{ts}, static pressure in the vicinity of the outlet of the secondary duct P_{si} and the secondary mass flow rate m_s. A primary-flow supersonic nozzle is placed on the centerline of the dect. Two types of the primary nozzle (Mach 2 nozzle and Mach 3 nozzle) whose exit height D is same were prepared. To change the area ratio of the secondary mixing duct area to the primary flow exit area, the height of the secondary flow duct is a variable. There are three types of mixing duct which have different length (L). To produce an aerodynamic-choking-condition downstream, a variable geometry nozzle is installed in the mixing duct. Geometrical features of the experimental setup are summarized in Table 1.

Figure 2 shows measurement items in the exeriments. Above the conditon parameters, the measured or obtained information is a set of wall pressure distributions, pitot sectional pressures and a Schlieren photograph of the mixing region.

Numerical Calculation

Numerical calculations were carried out with a commercial code GASP [10]. GASP is a finite volume flow solver with spacial discretisation. For the present computations, the two dimensional steady state Reynolds-Averaged Navier-Stokes (RANS) equations are solved with time marching. Roe's scheme with third order accuracy in both directions is employed for the flux-differencing together with Minimum Modulus limiting. The wall gradient calculation is performed with second order accuracy as well. As for the viscous fluxes, the thin layer terms are included in all directions, the cross derivative

Table 1 Geometrical features of the experimental setup.

Symbol	Notation	Range
D	Dimension of primary flow exit	30 [mm]
A_p	Primary flow exit area	30 [mm] x 50 [mm]
A_s	Secondary flow duct area	Variable
H_s	Duct Height	60 [mm] – 120 [mm]
L	Mixing duct Stream-wise length	400, 600, 800 [mm]

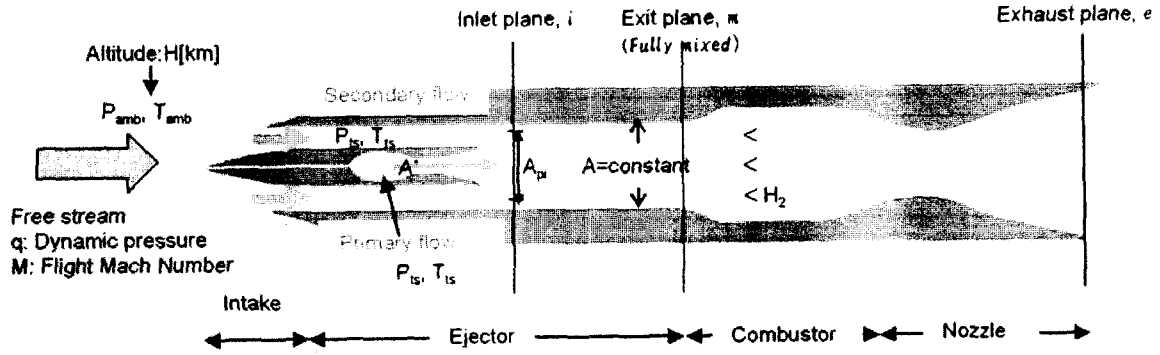

Figure 3. Conceptual diagram of a generic ejector-ramjet engine (notations are used in the flight performance analysis section).

terms are not included. To determine the laminar viscosity and thermal conductivity, Sutherland's law is applied. The binary coefficient and the mixture thermal conductivity are determined with constant Scmidt number of 0.7 and with the Wilke's relationship, respectively. To determine the turbulent coefficient of the thermal conductivity, a turbulent Prandtl number of 0.9 is used. A turbulent Schmidt number of 0.5 is used to determine the turbulent contributions of the mass diffusion coefficient. As a turbulence model, Wilcox's k-ω model is used. The computational domain covers the induction sections of the secondary duct and the primary nozzle and mixing duct, and the aft exit volume is prepared for inclusion of the ambient pressure boundary condition. The configuration is symmetric with z-x plane thus half of the domain is calculated. The grid consists of six blocks. For the inflow boundary conditions the stagnation conditions are fixed, in order to allow the velocity and therefore the mass flow to adapt. The outflow boundary condition is extrapolated for nozzle conditions and for other cases chamber pressure was given as back pressure. On all walls a no-slip adiabatic boundary condition is applied. The steady-state solutions are obtained with an implicit scheme. Gauss-Seidel time integration is used for external and internal iteration.

Analysis

Figure 3 shows a conceptual diagaram of a generic ejector-ramjet engine. The notation is based on the textbook by Heiser and Pratt [3].

There are typically two types of ejector ramjet cofigurations in terms of mixing and combution. One is Simultaneous Mixing and Combustion (SMC) and the other is Diffusion and Afterburning (DAB) [11]. Each has different merits and demerits. The SMC cycle has consistently lower specific impulse at low Mach number compared with DAB cycles but posesses simpler and possibly lighter structure. The DAB cycle may require a longer duct, but concerning utilization of the same duct path with the Ram and SCRam jet modes, this requirement is not a demerit. In this analytical study DAB cycle approach was chosen. As references, note that the SMC cycle was applied for simplified analyses by Billig [1] and Lentsch and coworkers [12].

The steady-state quasi-one-dimentional control volume concept is emplyed with numbers of assumption for the DAB cycle analysis in the textbook [3]. The analytical model was extended by Han and coworkets [13, 14, 15]. The present analytical configuration is based on these previous reports and there are several improvements on the original. The present approach and assumptions are explained in the following:

(1) Trajectory

During the flight, the hyposesis of a constant dynamic pressure path was chosen. In the program, dynamic pressure can be varied at any time. Combined with the atmospheric physical properties, flight Mach number is calculated. Ambient physical properties are taken from the US 1976 Standard Atmosphere altitude-pressure tables [16] with altitude information. Decision to the in-flight-condition is done with a threshold of incoming flow Mach number as 0.82. Below the Mach number, the incoming air Mach number is directly given by the user.

(2) Intake

For the intake pressure recovery determination, the MIL-E-5008B Specification [17] was used.

(3) Ejector core

The model of the ejector and the assumptions made for the analysis are summarized as following [3, 13]:

· The ejector has a constant area A and a fixed geometry.
· There are neither friction nor heat transfer near the duct wall.
· The secdondary flow is subsonic at the inlet plane.
· The primary flow is choked at its throat (area A^*) and it expands isentropically entraining the secondary flow by suction and viscous forces. Any shock waves created by the interaction of the two fluids are neglected.

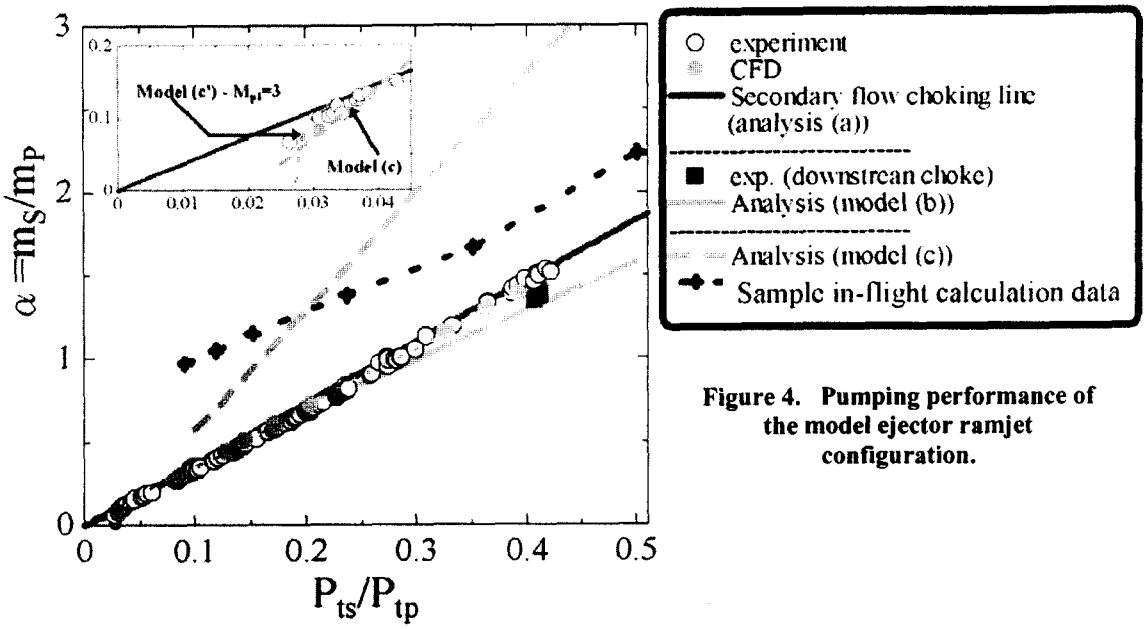

Figure 4. Pumping performance of the model ejector ramjet configuration.

· The mixing of the two fluids is completed at the ejector exit plane.
· The ejector exit plane is sonic or choked.

The entrainment and mixing calculation is progressed by finding an area ratio between the primary and secondary flows which attains the same static pressure. Simaltaneously mass, momentum and energy equations are solved for the adaption of the flow field. In addition to the above sequences, downstream occurrence of a weak normal shock can be employed so that the mixing loss term can be incorporated.

(4) Combustor

Only the reaction of hydrogen and oxygen into water vapor is taken into account. The assumption of the single-step chemistry is employed for comparison with the previous work. Adiabatic flame temperature calculation procedure or more realistic schemes can be replaced with the present assumption with the present model. Completion of the reaction and no losses are considered.

(5) Nozzle

A simple expansion calculation into the ambient air is employed without any losses.

After completion of the calculation, performance data are calculated such as specific impulse and the thrust augmentation factor.

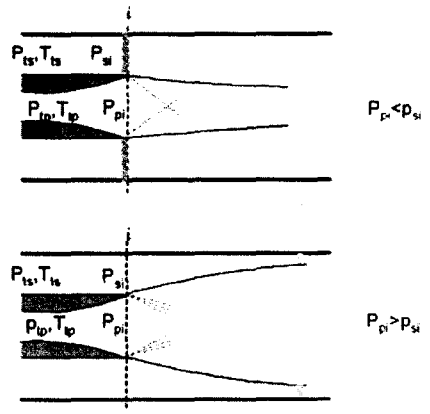

Figure 5. Two conditions of choking of the secondary flow: choking at the secondary duct exit (upper), choking in the freejet region (lower).

Results and Discussion

Flow Field Characteristics

Comprehensive reports on the experimental and numerical investigation were given in the previous work [7, 8]. In this paper, the pumping performance data is re-forcused and several comparisons with the present analysis are given. Figure 4 shows the relationship between the mass flow ratio of the secondary to primary flows $\alpha = m_s/m_p$ and total pressure ratio P_{ts}/P_{tp} for the condition shown in Table 2.

Table 2. Experimental Condition.

P_{tp}	0.4 [MPa]
T_{tp}	300 [K]
P_{ts}	Variable
T_{ts}	300 [K]
P_0	0.01 [MPa]
Hs	60 [mm], 70 [mm]
Primary flow Nozzle	Mach 3 Nozzle
Downstream Duct	Variable
L	400 [mm], 600[mm]

The experimental result (open circle) and the corresponding CFD result (solid circle) show that the mass flow ratio increases gradually, approaching to the secondary flow choking line (model (a)). For relatively small pressure ratio case the secondary flow is not choked. Those smaller pressure ratio conditions can occur when the relatively low speed or smaller dynamic pressure cases, in which conditions the ejector effect is most expected.

There are several flow-field patterns in the ejector configuration, but the most typical ones are pointed out into two, following Crocco [18]: one is secondary flow choking at the nozzle exit and the other is secondary flow choking in the free jet region. Secondary flow choking line is corresponds to the former one. The latter one can be evaluated by adoption of separated two flow configurations, which means that expansion of the primary exhaust flow narrows the secondary flow path resulting in the aerodynamic choking of the secondary flow in the mixing duct. Indeed Aoki and coworkers employed such an assumption to evaluate their experimental results. Figure 5 and Fig. 6 show the schematic notations of the flow feature based on reference 18.

From those results it is easy to find that the entrained secondary flow can be roughly classified into the above two. The former is attaied in the primary over expansion (OE) case (larger pressure ratio) and the latter one in the under expantion (UE) case (smaller pressure ratio).

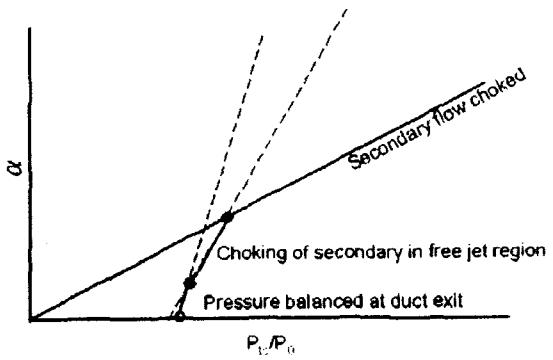

Figure 6. Secondary flow rate characteristics in the ejector pumping diagram.

Enlarged diagram for UE case is shown in a frame in Fig. 4. The model used in the flight-performance-analysis program is plotted (model (c)). This model shows similar trend to the experimental and CFD data. However, this line overpredicts the mass flow ratio for OE case, as will be discussed later. In the UE case, the primary flow closely expands to the designed pressure, a simpler model (model (c')) may be applicable. This is the model c with

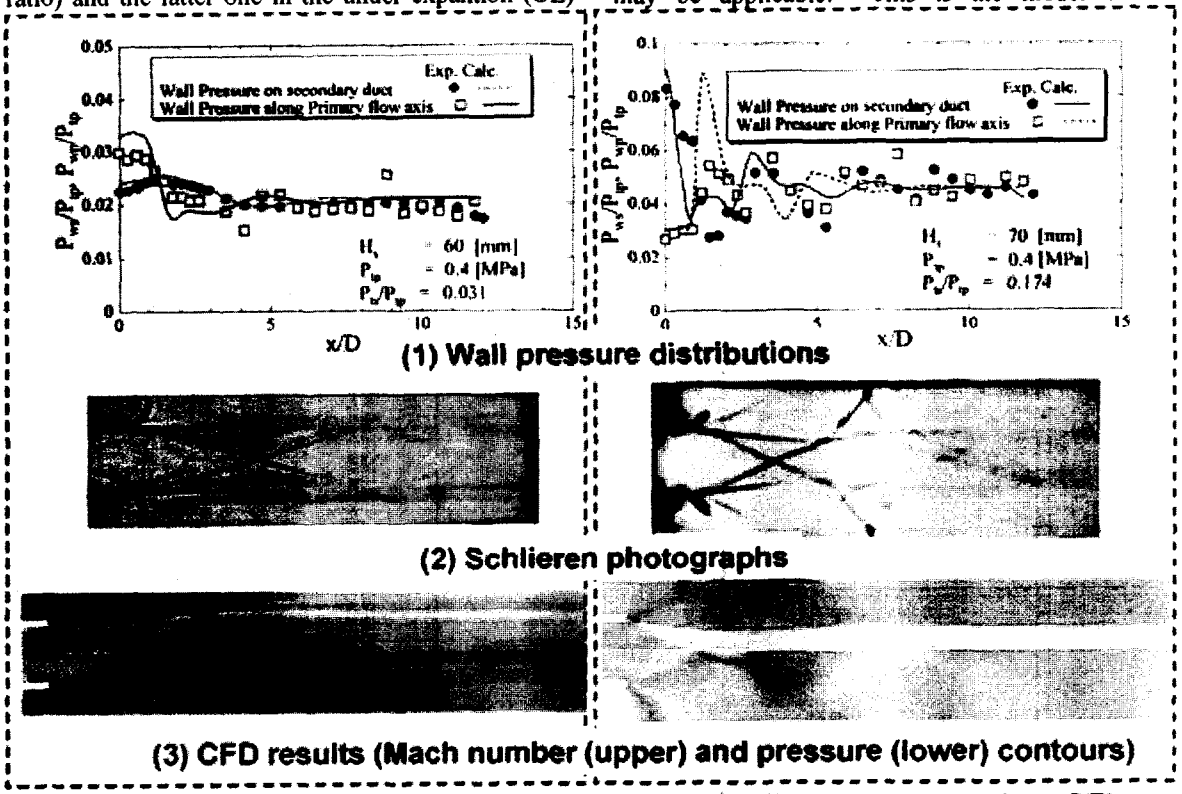

Figure 7. Experimental and CFD results of typical ejector flow-field features.

(a) Schlieren photograph from the experiment.

(b) CFD result (Mach number (upper) and pressure (lower) contours)

Figure 8. Downstream choking condition results.

application of the designed Mach number in the primary supersonic nozzle exit (mixing region inlet plane). The model by Aoki and coworkers predicts the values between models c and c'.

The above mentioned flow features can be examined by seeing the pressure distributions and the flow field. Figure 7 shows pressure distribution, Schlieren photograph image and corresponding CFD data for the above mentioned typical two cases (OE and UE cases). Figure 7-a shows the UE case and Fig. 7-b shows the OE case. From Fig. 7-b, attainment of the secondary flow choking at the nozzle exit is confirmed by the expansion wave at the exit. On the other hand, from Fig. 7-a aerodynamic choking during the mixing duct is confirmed in the CFD Mach number contour. The aerodynamic choking result was examied by separated two flow assumption with slipline by Aoki and coworkers [19]. Introduction of this assumption indicates lower mixing rate between the primary and secondary flows in this region. Figure 7 confirms that the assumption is valid in the present configuration.

Mixing enhancement is desired for shorter duct design. Simply enhancement of the primary and secondary flow can be attained by the occurrence of several weak obleque shock waves during the mixing (a more affirmative mixing enhancement would be attained by forming a robed supersonic primary nozzle to introduce stream-wise vortices [11, 20]. Experimental investigation of this mixing enhancement has been undergone for the present experimental configuration and the mixing enhancement was confirmed). In the practical engine operation, thermal choking may enhance some mixing by pressure rise. In this experimental configuration, similar downstream choking is attained by adopting a variable nozzle in the downstream of the mixing duct. Figure 8 shows sample Schlieren photograph and CFD result of the mixing duct choking condition, indicating occurrence of several oblique shock waves for better mixing. In Fig. 4, rectangle symbol shows the down stream choking result. The green line is an analytical solution assuming downstream choking with perfect mixing (model (b)). The resutlt shows good correspondence between the experiment and the analysis.

Also in Fig. 4, same assumption as used in the flight analysis program is applied for the experimental condition (model (c)). The result over-predicts the mass flow ratio for the OE case. This difference between the analysis and the experinent is caused by the secondary flow duct area confinement. The area information used in the analysis is primary flow throat area and the mixing duct area (equals to the summation of the primary and sedcondary exit areas). The calculation gives the secondary flow ratio without concering the secondary flow duct confinement. This indicates that the assumption of this model is insufficient and introduction of some simple flow field considerations above mentioned is required. For the application of the flow field models into the flight performance analysis program, it should be noted that the simpler and better prediction is desired. Although there are many 2 dimensional predictions for similar configurations available. (eg. References 4 and 19), careful decision of the utilization of experimental data, analytical predictions and CFD outputs should be made.

Table 3. Condition of sample air entrainment in flight.

Altitude	H=13.5 [km]
Dynamic pressure	q = 10-50 [kPa]
P_{tp}	0.4 [MPa]
T_{tp}	300 [K]
Area ratio	$A/A^* = 7.9$

Previous reports on the flight performance analysis varied many parameters separatedly, resulting in uncertain information from them. As an extreme example, a sample calculation of the flight analysis program adopting the cold flow experimental conditions was performed and the result is plotted in Fig. 4. The calculated condition is summarized in Table 3. As presented in the figure, flight performance analysis should carefully incorporate more precise flow field information.

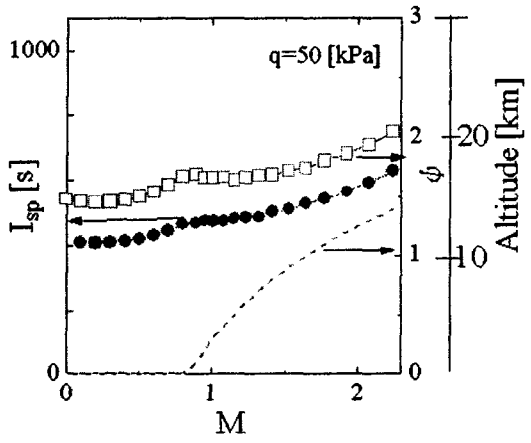

Figure 9. Flight performance sample output.

Table 4 Flight performance analysis condition.

Flight Mach number	0 – 2.3
Flight Dynamic Pressure	50 [kPa]
P_{tp}	5.0 [MPa]
T_{tp}	3500 [K]
Area ratio	$A/A^* = 7.9$
Intake Pressure Recovery	MIL-E-5008B
Ejector Mixing	Explained in the main body
Combustion	Energy addition through hydrogen-oxygen reaction
Nozzle	Expantion to ambient pressure

Flight Performance Analysis

After those considerations of the flow field and the flight performance analysis program, a sample flight performance analysis was conducted. The condition used in the calculation is summarized in Table 4. The result of the calculation is shown in Fig. 9. In the figure, altitude is plotted as dotted line. The thrust augmentation (defined as thrust divided by imaginary rocket alone thrust) and Isp is demonstrated. This program was also emplyed for the conditions in the previous reports and the validity of the code is confirmed. Although the present assumptions of ejector entrainment and mixing have shown some disparities from the in-detail flow features in terms of the mass flow rate, it can be understood that the present program serves as a bases for the acquisition of simplified flight characteristics comparable with the existing reports and for future incorporation of more precise flow features in it.

Concluding Remarks

In this paper, in order to construct a simplified method of the ejector flight performance analysis method, a corresponding flowfield data taken by the authors and the modifications to existing simple analytical procedure of the flight performance analysis were introduced and demonstrated.

For the ejector flow field insight, the ejector pumping performance was re-examined in the paper and the evaluation methods were examined. The information will be incorporated into the constructed simple flight performance analysis program.

As for the flight performance analysis, a simple analysis program was newly developed and it was confirmed that the present program output is in good correspondence with previous work and the present program serves as a bases for future incorporation of the more-in-detail flow features. After the examination of the problems solved in the new code, a sample flight performance result was demonstrated.

As the future study, more refined program will be provided and the systematic investigation will be performed.

Acknowledgements

The authors thank Juan Cantillo (Visiting student from SUPAERO, France), Shunji ENOMOTO, Masaharu KOH, Takuya MIZUNO, Yosinori HIRANO and Shizuo SEKINE for their help and advices during the study.

KO acknowledges the support of the Science and Technology Promotion Program under MEXT (Minixtry of Education, Culture, Sports, Science and Technology).

References

1) Billig, F. S., Low-Speed Operation of an Integrated Rocket-Ram-Scramjet for a Transatmospheric Accelerator, in Developments in High-Speed-Vehicle Propulsion Systems, Murthy, S. N. B. and Curran, E. T. Ed. , Progress in Astronautics and Aeronautics Volume 165, AIAA.

2) Kanda, T., Wakamatsu, Y., Sakuranaka, N., Izumikawa, M., Ono, F. and Murakami, A., Mach 8 testing of a scramjet engine with ramp compression, AIAA 2000-0616.

3) Heiser, W. H. and Pratt, D. T., Hypersonic airbreathing propulsion, AIAA Education Series.

4) Peters, C. E., Phares, W. J. and Cunningham, T. H. M., Thoretical and Experimental Studies of Ducted Mixing and Burning of Coaxial Streams, Journal of Spacecraft Vol 6., No. 12 pp. 1435-1441, 1969.

5) Kamhawi, H., Krivanek, T. M., Thomas, S. R. and Walker, J. F., Direct-Connect Ejector Ramjet Combustor Experiment, AIAA 2003-16, 2003.

6) 工藤、村上、苅田、加藤、複合サイクルエンジン燃焼試験 － スクラムジェットモード、日本流体力学会年会 2003 講演論文集、pp.492-493, 2003.

7) 岡井、田口、二村、エジェクタ・ラムジェット流れ場に及ぼす二次／一次流量比の影響、第 43 回航空原動機・宇宙推進講演会講演集、pp.351-356, 2003.
8) Okai, K., Taguchi, H. and Futamura, H., Experimental and Numerical Investigations of Ejector and Mixing Effects in a Model Ejector Ramjet Configuration, ISABE 2003-1230, 2003.
9) Taguchi, H., Sekine, S., Futamura, H., Yanagi, R, Omi, J. and Katoh, T., Verification test of Semi-Freejet Method for a Supersonic Engine Test Facility, AIAA 2000-3642.
10) Aerofost GASPex Users Manual, 1997.
11) Daines, R and Segal, C., Combined Rocket and Airbreathing Propulsion Systems for Space-Launch Applications, Journal of Propulsion and Power vol. 15 No. 5, pp. 605-612, 1998.
12) Lentsch, A., Taguchi, H., Shepperd, R. and Maita, M., Vehicle Concepts for an Ejector Ramjet Combined Cycle Engine, AIAA 2001-1793, 2001.
13) Han, S., Peddieson, Jr., J. and Gregory, D., Ejector Primary Flow Molecular Weight Effects in an Ejector-Ram Rocket Engine, Journal of Propulsion and Power Vol. 18, No. 3, pp. 592-599, 2002.
14) Han, S. and Tomes, J., A Numerical Study of Marquardt's Ejector-Scramjet Test Engine, AIAA 2002-3606.
15) Gregory, D. C. and Han, S., Effects of Multiple Primary Flows on Ejector Performance in an Ejector-Ram Rocket Engine, AIAA 2003-373, 2003.
16) United States 1976 Standard Atmosphere attitude-pressure tables.
17) MIL-E-5008B Specification.
18) Crocco, L., One-Dimensional Treatment of Steady Gas Dynamics, in Fundamentals of Gas Dynamics, High Speed Aerodynamics and Jet Propulsion Volume III Ed. Emmons, H. W., Princeton University Press, 1958.
19) Aoki, S., Lee, J., Masuya, G., Kanda, T., Kudo, K. and Murakami, A., Experimental Investigation of an Ejector Jet, AIAA 2003-188, 2003.
20) Lentsch, A., Morgenthaler, V. and Maita, M., CFD simulation of a rocket-ejector for an ejector-ramjet combined cycle engine, AIAA 2001-1863, 2001.